Unification of Strength Scaling between Unidirectional, Quasi-isotropic, and Notched Carbon/Epoxy Laminates

Xiaodong Xu[a*], Michael R. Wisnom[a], Kuan Chang[a] and Stephen R. Hallett[a]

[a]*Advanced Composites Centre for Innovation & Science (ACCIS), University of Bristol, University Walk, Bristol BS8 1TR, UK*

Abstract

An investigation into size effects and notch sensitivity in quasi-isotropic carbon/epoxy laminates was carried out. The purpose is to draw a complete picture of the strength scaling in unidirectional, quasi-isotropic, and notched carbon/epoxy laminates. A link was established between the strength scaling of the unidirectional and quasi-isotropic laminates. Efforts were made to understand the relationship between unnotched and open-hole strengths. For very small holes, the notched strengths approach the unnotched strength limit. A scaling law based on Weibull statistics was used to predict the unnotched laminate strengths. For very large holes, the same scaling law in conjunction with a detailed 3D ply-by-ply FE analysis with matrix cracks in the 90° plies and delamination cohesive interface elements was used to predict the large notched strengths. A good agreement between the modelling and experimental results was achieved. The effects of 90° matrix cracks on unnotched and notched strengths were also studied.

Keywords: A. Laminates; B. Strength; B. Stress concentrations; Scaling

* Corresponding author. Tel.: +44 (0)117 33 15098.
E-mail address: xiaodong.xu@bristol.ac.uk (X. Xu)

1. Introduction

Advanced composite materials have been widely used in the construction of large structures. To help assess the strength of composite components, the test pyramids for composite structures include a large amount of small coupons. To bridge the dimension gap between the laboratory coupons and the full-scale structures, it is necessary to understand size effects. A size effect can be defined as a change in strength with specimen dimensions [1]. Unnotched specimens of continuous fibre reinforced laminates have been extensively tested [2-6], emphasizing the volume-scaling effects. Unnotched quasi-isotropic specimens [3, 6] have also been tested to study the size effects, and free edge delaminations were identified to be one of the potential failure modes [6]. These free edge effects have been previously studied [7-9]. Free edges can give rise to stress concentrations due to high inter-laminar shear and normal stresses [10], as well as intra-laminar stresses in 90° plies [7]. In the case of quasi-isotropic laminates, free edge effects could potentially result in free edge delaminations prior to fibre breakage, which may lead to premature failure [6].

For the purposes of bolted connections, drilling into composites is inevitable. To better understand the phenomena of stress concentrations arising due to the introduction of different sized holes, the strength scaling in open-hole quasi-isotropic laminates under tensile loads has been investigated [11-14]. The hole diameters of the quasi-isotropic open-hole specimens were from 1 mm to about 50 mm. For intermediate sized holes (3.2 mm to 12.7 mm), sophisticated approaches [12, 15, 16] have been developed. It has been widely accepted that splits in the 0° plies can cause significant notch blunting [15, 17], and the magnitude of blunting increases with the split length [18, 19]. For very large holes (25.4 mm and 50.8 mm), it was found that the stress blunting effect

of the 0° splitting is eliminated, and the strength is asymptotic to a Weibull strength scaling line [13]. The implication is that the specimens need to be sufficiently large to be representative of the scaling behaviour at even larger sizes [13]. However, the previous Weibull strength scaling line was drawn through the point representing the largest open-hole specimens [13], and only its slope was predicted. Very small holes, less than 1 mm-diameter have not been studied before. The present study mainly focuses on the strength scaling in carbon/epoxy laminates with both very small and very large holes and the prediction of the magnitude as well as the scaling trend of the strength.

It has been shown that Weibull strength scaling theory applies for unidirectional (UD) laminates [1], and for large quasi-isotropic laminates with open holes [13], with the same Weibull modulus applicable in both cases. The current study demonstrates that the same Weibull strength scaling law also applies to unnotched quasi-isotropic laminates, and shows the relationship to the UD strength and scaling. It also demonstrates how the strength for large specimens with open holes can be predicted from the fundamental UD strength scaling, and how and why the strength of specimens with very small holes approaches the unnotched strength. This paper therefore aims to draw a complete picture of the strength scaling in unidirectional, quasi-isotropic, and notched carbon/epoxy laminates.

In the current study, length-scaled unnotched quasi-isotropic specimens are tested. Notched specimens with 0.5 mm and 1 mm diameter holes are also tested. The relationship between the unnotched strengths and the open-hole strengths is shown. For very large holes, once the unnotched tensile strength and Weibull modulus are measured from the independent UD laminate tests, the tensile strengths of the quasi-isotropic

laminates with large holes can be predicted with a detailed Finite Element (FE) analysis. For very small holes, it is shown experimentally that the notch sensitivity is largely reduced, and the open-hole tensile strengths of the quasi-isotropic laminates are expected to approach the predicted equivalent unnotched strength. Compared with other approaches, such as the average stress method, no curve fitting is required here. The scaling lines are drawn independently of the test results of the quasi-isotropic laminates. A good agreement between the predicted strengths and the experimental results is achieved, confirming that the proposed methods are applicable.

2. Test setup

In the present study, length-scaled unnotched tests are carried out to understand the size effects in quasi-isotropic laminates and the relation with UD strength scaling. The specimen lengths are scaled up by a factor of 2 and 4 as shown in Table 1.

Previously, open-hole specimens were tested [11]. A schematic of the specimens (D = 3.2, 6.4, 12.7 and 25.4 mm) with their in-plane dimensions scaled up by up to a factor of 8 is shown in Figure 1. The hole diameter-to-width ratio was kept constant (0.2) for the previous specimens. A larger Scale 16 open-hole specimens (D = 50.8 mm) was also tested [13], with only the width and hole diameter of the specimen being scaled up, while the gauge length was kept the same as the one-size-smaller Scale 8 specimen (D = 25.4 mm). This was due to the limitations of the testing and manufacturing facilities. Tests and FE analysis showed that the use of the relatively shorter specimens did not affect the results [13]. In the present study, another two sets of specimens with smaller holes, the Scale 0.5 (D = 0.5 mm) and Scale 1.0 (D = 1.0 mm), are tested. The holes were drilled with 0.5 mm Tungsten Carbide drill bits and 1.0 mm EMCTIALN Carbide TiAlN end mills. Their in-plane dimensions were kept the same as in the

previous baseline specimen (D = 3.2 mm), in order to reduce the influence of the free edges on the stress distribution around the hole. The dimensions of all of the specimens are summarized in Table 2. The hole diameters are consequently scaled up by up to a factor of about 100 from the smallest to the largest specimens.

The material used in all these tests is Hexcel HexPly® IM7/8552 carbon/epoxy pre-preg with a nominal ply thickness of 0.125 mm. The stacking sequence of all the specimens is quasi-isotropic $[45/90/-45/0]_{4s}$. The nominal overall thickness is 4 mm, which is very close to the actual specimen thickness. Hydraulic-driven test machines were used to test the specimens under displacement control. Loading rates were scaled with regards to the specimen gauge length. Interrupted tests in which the tests were stopped at 95 % of the average failure load were carried out for some specimens. The specimens from the interrupted tests were examined by X-ray Computed Tomography (CT scanning) to study the damage state close to failure. The samples from the interrupted tests were soaked in a bath of zinc iodide penetrant for 3 days. A Nikon XT H 225ST CT scanner was used. It has proprietary 225 kV microfocus X-ray source equipped with a reflection target, offering a 3 μm focal spot size.

It was previously reported that unnotched quasi-isotropic specimens failed away from the end tabs [6]. However reassessment of the specimens showed that while gross failure occurred in the gauge section, there were transverse cracks and delaminations initiating at the tabs. The glass/epoxy composite end tabs previously used have vertical edges near the carbon/epoxy laminates. Additionally, defects such as voids were present in the epoxy fillets at the corners of the glass/epoxy composite end tabs. Consequently, stress concentrations were introduced to the specimens due to the geometrical discontinuity at the end tabs and the defects within the epoxy fillets. Some transverse

surface cracks starting at the end tabs were found by dye penetrant testing (Ardrox 9812) of a previous 32 mm × 120 mm $[45/90/-45/0]_{4s}$ unnotched specimen from an interrupted tests (95 % of the average failure load) as shown in Figure 2. In order to avoid this, no end tabs were used in the current study, and the specimens were gripped directly in the test machine jaws. The steel grips of the test machine have a very gradual chamfer at the ends, which is designed to reduce gripping stress concentrations.

3. Experimental results

3.1. Previous unnotched tests of UD laminates

Previously, 3D volume-scaled unnotched UD laminates have been tested under tensile loads [6]. The failure of the specimens was dominated by fibre breakage, which can be interpreted by a weakest-link model and Weibull distribution [20]. A significant size effect was found, with a 14 % reduction in unnotched strength of IM7/8552 for an 8 times increase in linear dimensions, corresponding to a Weibull modulus of 41 [6]. The Weibull modulus, and the unnotched strength extracted from these unnotched UD tests will be referred to later in the present study.

3.2. Previous open-hole tests of quasi-isotropic laminates

Previously, in-plane scaled open-hole quasi-isotropic laminates have been tested under tensile loads [11, 13]. A significant size effect was found, with a 32 % reduction in notched strength of IM7/8552 for a 16 times increase in linear dimensions. It was also found that for specimens with hole diameters larger than 25.4 mm, the strength is asymptotic to a Weibull strength scaling line for circular holes [13], with the same Weibull modulus as that extracted from the unnotched UD tests [6]. However, only the slope of the strength scaling line was studied, and the scaling line was drawn through the point representing the largest open-hole test results (D = 50.8 mm). The relation of

the notched strength to the unnotched UD parameters as well as the magnitude of the size effects are investigated in the present study.

3.3. Length-scaled unnotched tests of quasi-isotropic laminates

In the current study, length-scaled unnotched quasi-isotropic laminates have been tested under tensile loads. All load vs. cross-head displacement responses in the current length-scaled unnotched tests were approximately linear. No obvious damage was seen with the naked eye before final failure. The final failure was catastrophic in all the tests, and the dominant failure mode was fibre failure. The highest load level was taken as the failure load, from which the unnotched strengths were calculated. 8 specimens with gauge length failures of each size were included in the calculation. The unnotched strengths of the length-scaled quasi-isotropic specimens are shown in Table 3. The Weibull modulus in Table 3 is extracted from the least squares fit on the log-log plot in Figure 3. There is a 3.4 % reduction in unnotched strength for a 4 times increase in linear dimensions. The size effect is statistically significant at a significance level of 1% in a one tailed Student's t-test, the standard statistical test used to demonstrate that the strength values for two sets of results are statistically different.

The gripping compression suppresses edge delamination within the grips, which can reduce or eliminate premature damage near the end tabs in the current study. As a result, few specimens suffer from failures near the end tabs. All specimens were carefully examined and any tab failures excluded. The unnotched strengths of the tested quasi-isotropic laminates achieved (within 1.5 %) the same value as calculated from the UD tests according to Classical Laminate Theory (CLT) and an appropriately scaled strength for the whole volume of the 0° plies, as shown in Table 3. Thermal residual stresses would have a small effect on these results, but for simplicity are not included

here. The fact that the average unnotched strength of the previous specimens was lower and had larger scatter [6] is because of the transverse surface cracks starting at the end tabs, which were avoided in the current tests.

3.4. Small open-hole tests of quasi-isotropic laminates

In the present study, quasi-isotropic laminates with holes of 0.5 mm and 1.0 mm have been tested under tensile loads. All load vs. cross-head displacement responses in the open-hole tests were initially linear, then slightly softened due to subcritical damage. The final failure was catastrophic in all the tests. The highest load level was taken as the failure load from which the notched strengths were calculated by using the measured full widths and the nominal thickness of the specimens. The open-hole strengths for all sizes including the previous test results are summarized in Table 4. Because the smaller specimens have a different notch-to-width ratio, the small open-hole strengths are converted to equivalent values for a notch-to-width ratio of 0.2 according to Equation 1 in order to be comparable with the previous specimens. The finite-width correction factor, $f(\lambda)$, is calculated based on the finite-width corrected Stress Concentration Factor (SCF) from Equation 2 [21] which is strictly accurate only for the elastic range, but is used here to at least partially correct for this effect even though it is small.

$$\sigma_{\text{eq}} f(0.2) = \sigma_{\lambda} f(\lambda) \tag{1}$$

$$f(\lambda) = \frac{K_T}{K_T^{\infty}} = \frac{3 - 3.14(\lambda) + 3.667(\lambda)^2 - 1.527(\lambda)^3}{3(1-\lambda)} \tag{2}$$

where λ is the notch-to-width ratio, σ_{eq} is the equivalent strength at λ = 0.2, σ_{λ} is the measured strength, K_T is the finite-width corrected SCF (when λ = 0.2 for the larger holes, K_T = 3.13), and the SCF for infinitely wide specimens is K_T^{∞} = 3.00. $f(\lambda)$ remains close to unity, e.g. $f(\lambda)$ = 1.00 for very small holes and 1.04 for the larger holes.

4. Results analyses

The unnotched strength of UD laminates was previously found to scale with the volume of specimen, and can be described through the Weibull strength scaling theory (Section 4.1). This can then be linked to the strength of unnotched quasi-isotropic laminates of the same material through an equivalent strength based on CLT and the whole volume of the 0° plies (Section 4.2). It might be expected that the open-hole strength could be predicted through the same Weibull strength scaling theory, but this is shown not to work (Section 4.3). One potential reason for this is the free edge effect, but this is shown not to explain the discrepancy (Section 4.4). Another potential explanation is the effect of 90° matrix cracks (Section 4.5). Matrix cracks in the 90° plies are simulated in a detailed model (Section 4.6). With the detailed model, the notched strength scaling of large holes can be linked to the unnotched strengths (Section 4.7). Finally, the notched strength scaling of both very small and very large holes can be unified by the stress blunting effects of 0° splitting (Section 4.8). A unified view about strength scaling is therefore presented - a Weibull strength scaling integration over the stressed volume is applicable to all configurations, and careful consideration of the effect of 90° matrix cracks can improve the predictions.

4.1. Scaling of unnotched strengths of UD laminates

Larger composite laminates are more likely to have a larger defect, leading to lower strength. Wisnom [1] applied a two-parameter Weibull distribution, in which the probability of survival, $P(s)$, of a volume V subject to a stress σ is,

$$P(s) = \exp[-V(\sigma/\sigma_0)^m] \tag{3}$$

where σ_0 is the characteristic strength of material, and m is the Weibull modulus.

By assuming equal probability of survival, the strength of a specimen σ_1, with stressed volume V_1 can be related to the strength of another specimen σ_2, with stressed volume V_2, according to Equation 4.

$$\sigma_1 / \sigma_2 = (V_1 / V_2)^{-1/m} \quad (4)$$

We can derive σ_{unit} = 3131 MPa, the tensile strength of a unit volume of UD IM7/8552 carbon/epoxy material [15] and a Weibull modulus of m = 41 from volume-scaled unnotched UD tests [6]. By using σ_{unit} = 3131 MPa as the characteristic strength and m = 41 as the Weibull modulus of the material, the strength of UD material σ_{UD} with volume V_{UD} is therefore given by Equation 5.

$$\sigma_{UD} = \sigma_{unit} V_{UD}^{-1/m} \quad (5)$$

4.2. Relation between UD strength and quasi-isotropic strength

It should be possible to predict the strength of unnotched quasi-isotropic laminates by comparing the main load-carrying 0° ply stress from CLT with the volume adjusted unnotched strength of the 0° plies σ_{UD}. Taking the short-unnotched specimen for example, the volume of the specimen is known, a quarter of which is 0° plies. σ_{UD} = 2644 MPa, calculated according to Equation 5, which is the volume adjusted strength of the 0° plies. The predicted equivalent strength is therefore σ_{UD} / 2.61 = 1012 MPa, where 2.61 is the ratio between the stress in the 0° plies and that in the whole laminate according to CLT. The measured unnotched strengths from the length-scaled tests are within 1.5 % of the equivalent strengths predicted in this way, as shown in Table 3. The Weibull modulus extracted from the length-scaled quasi-isotropic tests is 40, almost the same as the value of 41 from the volume-scaled UD tests [6]. This means that fibre breakage in the 0° plies dominates the failure of length-scaled unnotched quasi-isotropic laminates. In fact, the length-scaling problem is a volume-scaling problem for the unnotched quasi-

isotropic laminates. This finding completes the previous study of size effects in unnotched quasi-isotropic laminates [7], in which the unnotched tests results were affected by failures near the end tabs, so there were not enough data to draw the same conclusion.

4.3. Predicting large open-hole strengths assuming no damage

3D ply-by-ply linear elastic FE modelling using the explicit code LS-Dyna is applied to determine the stress distribution in the previous Scale 8 open-hole specimen (D = 25.4 mm) assuming no damage. The FE analysis is done on the Scale 8 specimens instead of the largest Scale 16 specimens, in order to see if the current approach could be used as a prediction tool for even larger hole sizes based on a relatively smaller model (with fewer elements). As demonstrated in the previous study [13], the experimental results already start to fall on the notched strength scaling line within the experimental scatter from the Scale 8 specimens onwards. The Scale 8 specimens are therefore believed to be large enough for the prediction of even larger specimens. However this assumption does not affect the results presented in this section since the model does not include any damage, so the stress results will be independent of model size.

8-node constant-stress solid elements are used with one element through each ply thickness. The FE results were compared with those with two elements through each ply, and they differ by less than 2.0 %. As a result, only one element through each ply thickness is used in all of the following FE analyses. Half of the Scale 8 open-hole specimen is modelled through the specimen thickness. Uniform displacements are applied to one end of the model and the nodes are fixed at the other end. Symmetry boundary conditions are applied at the mid-plane through the specimen thickness. The baseline mesh of the Scale 8 model has a minimum mesh size of about 0.04 mm at the

hole edge. The refined mesh transitions to a coarser mesh away from the hole edge. In the FE analyses, material properties are the same for all cases, as shown in Table 5 [15]. The mass was scaled up by a factor of about 10,000 in all FE models. Dynamic effects were checked to be sufficiently low so as not to affect the results. A -160°C temperature drop is applied before mechanical loading, in order to generate the thermal residual stresses formed during curing.

A failure criterion based on Weibull strength scaling theory has been used to predict fibre failure [22]. The idea is to sum the elemental contributions to the probability of failure as functions of both the volume and the stress level through a Weibull integration. Starting from Equation 3 and assuming equal probability of survival, the right hand integral can be replaced numerically by a summation over the elements of the FE model to give Equation 6. Equation 6 can be rearranged to become Equation 7 as a fibre failure criterion which is checked at each time step in the explicit FE analyses.

$$\exp[-(\sigma_{\text{unit}}/\sigma_0)^m] = \exp[\sum_{i=1}^{\text{Total Number of Elements}} -V_i(\sigma_i/\sigma_0)^m] \quad (6)$$

$$\sum_{i=1}^{\text{Total Number of Elements}} V_i(\sigma_i/\sigma_{\text{unit}})^m = 1 \quad (7)$$

where σ_i is the elemental stress, V_i is the volume of the element i, σ_{unit} = 3131 MPa is the tensile strength of unit volume UD material, and σ_0 is the characteristic strength of the material, which cancels out.

When Equation 7 is satisfied, the point of fibre failure has been reached. The element with the maximum stress is marked as the weakest-link, which triggers ultimate failure. The stress distribution just before the ultimate failure is determined in a Scale 8 open-hole model (D = 25.4 mm), and the predicted strength is the applied far-field stress at that point. The open-hole strength of the previous Scale 8 specimens is predicted as σ_f =

365 MPa. The FE results are compared with those with doubled minimum mesh size (about 0.08 mm compared with 0.04 mm) at the hole edge. The results differ by less than 1.0 %, showing that they are not sensitive to the mesh size. The FE model over-predicts the open-hole strength (experimental = 331 MPa, C.V. 3.0 %) of the Scale 8 specimens by about 10 %.

4.4. Effect of free edges in unnotched model assuming no damage

One possible reason for the above discrepancy between the numerically predicted strength and the experimentally measured strength is free edge effects. 3D free-edge effects on the loading-direction stress distribution are studied in a short (63.5 mm-long) unnotched ply-by-ply linear elastic FE model which is similar to that described in Section 4.3. The model has a minimum mesh size of about 0.05 mm near the free edges. The loading-direction stress distribution across the model width near the free edge is illustrated in Figure 4. The loading-direction stress decreases in the 0° plies at the free edge by 2.5 %, and increases in the 90° plies by 29 % , which agrees with the trend found in previous literature [7]. This is because the mechanical strain in the loading direction (0° in the current study) in the 90° plies is equal to the total strain minus the strain introduced by the Poisson's effects. Due to Poisson's effects, the 90° plies are compressed across the specimen width, so the 'Poisson's strain' in the loading direction is generally positive in the 90° plies. But at the free edges, 90° plies are free from compression, so the 'Poisson's strain' is zero. Therefore the mechanical strain and associated stress in the loading direction increases at the free edges in the 90° plies, but decreases in the 0° plies. This free edge effect only occurs within about one ply thickness (0.125 mm) from the free edges. Because the stresses within the 0° plies

decrease at the free edges, the free edge effects cannot explain the over-prediction of the open-hole strength.

4.5. Effect of matrix cracks in the 90° plies on unnotched strength

In the quasi-isotropic specimens, matrix cracking in the 90° plies are commonly observed across the whole specimen width as shown in Figure 5. This is due to the low transverse strength of the 90° plies. With the presence of 90° matrix cracks, the loading-direction stress in the 90° plies has to be transferred to the adjacent plies including the 0° plies. This effect is enhanced because the stresses in the 90° plies are increased at the free edges, as demonstrated in Section 4.4.

The 3D ply-by-ply FE modelling in Section 4.4 is therefore updated to take account of the 90° matrix cracks. Cohesive interface elements are pre-defined between adjacent plies to simulate inter-laminar damage. The properties of the cohesive interface elements are shown in Table 6 [15]. The mixed-mode traction displacement relationship for cohesive interface elements is illustrated in Figure 6 [23]. Three open matrix cracks across the full model width are pre-defined within each 90° ply to simulate the matrix cracks emanating from the free edges and their interaction as shown in Figure 7. The previous short unnotched model had the same gauge length as the short unnotched specimens, but the boundary conditions introduce artificial stress concentrations. It is also not practical to pre-define all the potential 90° matrix cracks along the gauge length. To resolve the above issues, the current short (63.5 mm-long) unnotched model only contains three matrix cracks within each 90° ply in the middle of the gauge section, so they are far from the model boundaries. Models with different matrix crack spacing are compared, so that the interaction between the matrix cracks could be investigated. The elements near the inner 90° matrix crack in the 0° plies are regarded as a unit strip. Their

loading-direction stress distribution is assumed to repeat itself over the whole gauge length to represent the overall stress distribution in the 0° plies with multiple uniformly spaced 90° matrix cracks. In this case, the Weibull integration (Equation 7) is done through post-processing the results in the region of the matrix cracks and taking account of the number of such regions that would occur along the length of a full specimen if one assumes a uniform crack density. The initial applied stress in the model is chosen to be close to the expected unnotched strength, then is linearly interpolated and iterated until Equation 7 is met. No ±45° and 0° splits are modelled, because they were not observed in the CT scanning images of the unnotched specimens.

The FE results were compared with those with doubled minimum mesh size (0.1 mm) near the free edges. The results only differ by less than 0.2 %, showing they are not mesh-size dependent. The FE results with 0.8 mm crack spacing, which is to the same order of the experimentally observed spacing, are compared to those with doubled crack spacing, and the difference is only 0.7 %. The combined influence from free edges and 90° matrix cracks is therefore not affected by the crack spacing. Consequently, only one matrix crack will be used in each 90° ply in the updated open-hole model as shown in Figure 8 in the next section.

The detailed 3D FE analysis with 90° matrix cracks across the full model width (minimum mesh size of 0.05 mm) confirms a slight stress concentration near the free edges in the short unnotched specimen as illustrated in Figure 9. The loading-direction stress in the 0° plies at the free edges is higher by about 4.0 % compared with the background stress in the middle of the model. Because in the unnotched model assuming no damage in Section 4.4 the loading-direction stress in the 0° plies is 2.5 % lower at the

free edges than that away from the free edges, the 90° matrix cracks introduce an additional stress concentration of about 6.5 % in the 0° plies at the free edges.

The FE prediction of the unnotched strength of the short quasi-isotropic specimen based on integrating the stresses in the 3D model with uniform matrix crack spacing of 0.8 mm is 987 MPa. This is within 2.5 % of the predicted equivalent unnotched strength of 1012 MPa according to CLT and the whole volume of the 0° plies calculated in Section 4.2. The stress concentration introduced by the 90° matrix cracks does not significantly affect the unnotched strength, because the volume affected by the stress concentration is small compared with the whole volume of the specimen. Hence the Weibull integral in Equation 7 is dominated by the contribution of the bulk of the specimen subject to the nominal stress. This explains why a good prediction of laminate strength was obtained previously without taking account of the 90° matrix cracks.

4.6. Effects of matrix cracks in 90° plies on notched strength

Unlike the detailed unnotched model, the updated Scale 8 open-hole model with 90° matrix cracks across the full model width in Figure 8 (with minimum mesh size of about 0.04 mm) shows that the stress concentration due to the matrix cracks does affect the predicted open-hole strength. This is because the stress concentration introduced by the 90° matrix cracks coincides with the stress concentration introduced by the circular hole. The updated Scale 8 open-hole model with 90° matrix cracks predicts a notched strength of σ_f^* = 343 MPa from Equation 7. This is about 6.0 % lower than the predicted notched strength without considering the 90° matrix cracks. The FE results are compared with those with doubled minimum mesh size (about 0.08 mm) near the hole edge. The coarse-mesh prediction is within 3.0 % of the baseline fine-mesh prediction, so the results are only slightly mesh-size dependent.

The predicted notched strength reduction of about 6.0 % is close to the additional stress concentration of about 6.5 % introduced by the 90° matrix cracks at the free edges in the unnotched model (which effectively corresponds to an infinitely-large hole) in Section 4.5. This indicates that for holes larger than 25.4 mm, the additional stress concentration introduced by the 90° matrix cracks does not depend on the hole size. This is because the free edge effect only affects the elements within roughly one ply thickness (0.125 mm) around the hole, which is relatively small compared to the larger hole diameters. As a result, the stress distribution for larger holes should be similar to that in the Scale 8 model with 90° matrix cracks, justifying the use of this sized model in the current analysis. For small holes, there may be some interaction with the free edge, so the diameter may affect the stress concentration. However, there will be subcritical damage at the hole edge, so the stress concentration will also be affected by the amount of delamination and splitting in other plies, as has already been demonstrated by Hallett et al. [15].

4.7. Scaling of open-hole strengths of quasi-isotropic laminates

The failure of unnotched quasi-isotropic laminates is controlled by defects generally evenly distributed within the whole volume of 0° plies as demonstrated in Section 4.1. In contrast, the failure of the open-hole specimen is controlled by the same defects distributed in the 0° plies around the hole boundary where there are stress concentrations. As the hole diameter scales up, the volume of stressed material scales up with it. As a result, the tensile strengths of the scaled-up open-hole specimens decrease according to the Weibull strength scaling theory which is represented by Equation 4.

For very large open-hole specimens, the Weibull strength scaling line in Figure 10 is drawn independently of the notched test results, with its magnitude predicted

numerically from the Scale 8 open-hole model (σ_f^* = 343 MPa), and with its slope determined by Equation 4 and the Weibull modulus m = 41. The tensile strength of the even larger Scale 16 specimens is well predicted, as shown in Figure 10. This is because delamination from ply cracks is greatly inhibited for large holes [24], and the subcritical damage such as 0° splitting is almost eliminated. What is more, the additional stress concentration introduced by 90° matrix cracks does not depend on the hole size for very large holes. Consequently, the total stress concentrations are approximately the same for different sized large holes.

For very small open-hole specimens, the stress blunting effect of zero ply splitting is so great that the notched strength is expected to approach the unnotched strength limit as shown in Figure 11. The upper limit is the predicted equivalent unnotched strength from Section 4.2 with uniform stress distribution and the same volume of 0° plies as the notched specimens. Because the three sets of specimens in Figure 11 share the same overall dimensions as the unnotched specimens, the upper limit is a constant value of 1012 MPa. The unnotched strength limit line is not based on the length-scaled unnotched tests, but derived independently from the volume-scaled UD tests.

4.8. Stress blunting effects of 0° splits

The scaling of notch sensitivity can be explained by a unified mechanism, which is the stress blunting effects of the 0° splitting. The stress blunting effects can be quantified by a normalized 0° split length L_N, which is defined as the total central 0° split length in both directions at one side of the hole edge divided by the hole diameter. There is splitting in all 0° plies, and the central 0° splitting is chosen as representative. Delamination was not observed prior to ultimate failure except at surface plies, neither was there any obvious fibre breakage.

The same points in Figure 11 are rearranged with regard to their L_N in Figure 12. For very large holes ($L_N \rightarrow 0$, the limit is no 0° splits), the stress distribution around the large holes is similar to that without the stress blunting effects of the 0° splits, and the open-hole strength therefore reaches the lower limit of the numerically predicted notched strength. A Strength Reduction Factor (SRF) of 2.66 can be calculated by dividing the predicted equivalent unnotched strength (1012 MPa) by the predicted notched strength (380 MPa) without 0° splitting and associated stress blunting. The numerically predicted notched strength of 380 MPa is derived from the predicted notched strength of 343 MPa of the Scale 8 model (D = 25.4 mm) with 90° matrix cracks, increased according to Equation 4 (m = 41) and the smaller volume of the 0° plies in the baseline specimen (D = 3.2 mm). This calculated SRF is smaller than the theoretical SCF value of 3.13 (λ = 0.2) for a circular hole, because the stressed volume at the hole edge is smaller than the volume of the whole specimen. A volume correction factor can be defined as the ratio of the uniform stress over the whole volume of the specimen to the peak stress at the hole edge giving equal probability of survival, and is calculated to be 0.85 by integrating the stress distribution using Equation 7. The calculated SRF of 2.66 is therefore equal to the theoretical SCF of 3.13 times the volume correction factor of 0.85. For very small holes ($L_N \rightarrow \infty$, the limit is infinitely-long 0° splits), the stress concentration affects a decreasing volume and the strength would be expected to approach the limit of the uniformly stressed unnotched specimens. The upper limit of the open-hole strength is therefore the predicted equivalent unnotched strength of 1012 MPa.

5. Conclusions

Length-scaled unnotched quasi-isotropic laminates and in-plane scaled large open-hole quasi-isotropic IM7/8552 laminates follow the same Weibull strength scaling

law as volume-scaled unnotched UD laminates. They all share the same Weibull modulus and scale parameters. This is because the failure of all the configurations is fibre dominated, and is controlled by the same defects distributed over the stressed volume.

Matrix cracks in 90° plies introduce a slight stress concentration in the 0° plies of quasi-isotropic laminates but the effect is negligible except near free edges and hole boundaries. The stress concentration does not significantly affect the unnotched strength, because the associated volume at the free edges is small compared with the whole specimen volume. However, the slight stress concentration does affect the notched strength because it coincides with the geometrically introduced stress concentration in the vicinity of the hole.

The failure of the open-hole specimens is controlled by defects distributed within the stressed volume at the hole boundary. The large open-hole tensile strengths can be related to the unnotched strength in a detailed 3D ply-by-ply FE analysis with 90° matrix cracks and delamination cohesive interface elements. For holes of at least 25.4 mm, the notch sensitivity is approximately constant, but the reduction in strength is smaller than the theoretical SCF. This is because the stressed volume of the 0° plies around the hole is smaller than the whole volume of the 0° plies. The Weibull strength scaling line for notched quasi-isotropic laminates which is derived from the UD data and the detailed FE analysis yields quite a good prediction for the 25.4 mm and even larger 50.8 mm open-hole tests. For smaller holes, the stress blunting effect is substantial as the relative split length increases. The strength follows the expected trend towards the limit based on the predicted equivalent unnotched strength according to CLT and the whole volume of the 0° plies.

References

[1] Wisnom MR. Size effects in the testing of fibre-composite materials. Composites Science and Technology. 1999;59(13):1937-57.

[2] Humer K, Tschegg EK, Weber HW, Noma K, Yasuda J, Iwasaki Y. Specimen size effect on tensile-strength of 3-dimensionally glass-fibric reinforced-plastics at room and cryogenic temperatures. Cryogenics. 1993;33(2):162-8.

[3] Johnson DP, Morton J, Kellas S, Jackson K. Scaling effects in sublaminate-level scaled composite laminates. AIAA Journal. 1998;36(3):441-7.

[4] Sutherland LS, Shenoi RA, Lewis SM. Size and scale effects in composites: II. Unidirectional laminates. Composites Science and Technology. 1999;59(2):221-33.

[5] Lavoie JA, Soutis C, Morton J. Apparent strength scaling in continuous fiber composite laminates. Composites Science and Technology. 2000;60(2):283-99.

[6] Wisnom MR, Khan B, Hallett SR. Size effects in unnotched tensile strength of unidirectional and quasi-isotropic carbon/epoxy composites. Composite Structures. 2008;84(1):21-8.

[7] O'Brien TK. Characterization of delamination onset and growth in a composite laminate. Damage in Composite Materials, ASTM STP 775. 1982(140):140-67.

[8] Sun CT, Zhou SG. Failure of quasi-isotropic composite laminates with free edges. Journal of Reinforced Plastics and Composites. 1988;7(6):515-57.

[9] Xu X, Wisnom MR. An experimental and numerical investigation of the interaction between splits and edge delamination in [+20m/-20m]ns carbon/epoxy laminates. 15th European Conference on Composite Materials. Venice, 2012.

[10] Jones RM. Mechanics of composite materials. 2nd ed: Taylor & Fransis; 1998.

[11] Green BG, Wisnom MR, Hallett SR. An experimental investigation into the tensile strength scaling of notched composites. Composites Part A: Applied Science and Manufacturing. 2007;38(3):867-78.

[12] Camanho PP, Maimí P, Dávila CG. Prediction of size effects in notched laminates using continuum damage mechanics. Composites Science and Technology. 2007;67(13):2715-27.

[13] Xu X, Wisnom MR, Mahadik Y, Hallett SR. An experimental investigation into size effects in quasi-isotropic carbon/epoxy laminates with sharp and blunt notches. Composites Science and Technology. 2014;100(0):220-7.

[14] Furtado C, Arteiro A, Catalanotti G, Xavier J, Camanho PP. Selective ply-level hybridisation for improved notched response of composite laminates. Composite Structures. 2016;145:1-14.

[15] Hallett SR, Green BG, Jiang WG, Wisnom MR. An experimental and numerical investigation into the damage mechanisms in notched composites. Composites Part A: Applied Science and Manufacturing. 2009;40(5):613-24.

[16] Camanho PP, Erçin GH, Catalanotti G, Mahdi S, Linde P. A finite fracture mechanics model for the prediction of the open-hole strength of composite laminates. Composites Part A: Applied Science and Manufacturing. 2012;43(8):1219-25.

[17] Kortschot MT, Beaumont PWR. Damage mechanics of composite materials: I—Measurements of damage and strength. Composites Science and Technology. 1990;39(4):289-301.

[18] Kortschot MT, Beaumont PWR, Ashby MF. Damage mechanics of composite materials. III: Prediction of damage growth and notched strength. Composites Science and Technology. 1991;40(2):147-65.

[19] Xu X, Wisnom MR, Li X, Hallett SR. A numerical investigation into size effects in centre-notched quasi-isotropic carbon/epoxy laminates. Composites Science and Technology. 2015;111(0):32-9.

[20] Weibull W. A statistical distribution function of wide applicability. Journal of Applied Mechanics. 1951;18:293-7.

[21] McGinty B. Stress concentrations at holes. 2014. http://www.fracturemechanics.org/hole.html

[22] Li X, Hallett SR, Wisnom MR. Numerical investigation of progressive damage and the effect of layup in overheight compact tension tests. Composites Part A: Applied Science and Manufacturing. 2012;43(11):2137-50.

[23] Jiang W-G, Hallett SR, Green BG, Wisnom MR. A concise interface constitutive law for analysis of delamination and splitting in composite materials and its application to scaled notched tensile specimens. International Journal for Numerical Methods in Engineering. 2007;69(9):1982-95.

[24] Wisnom MR, Hallett SR. The role of delamination in strength, failure mechanism and hole size effect in open hole tensile tests on quasi-isotropic laminates. Composites Part A: Applied Science and Manufacturing. 2009;40(4):335-42.

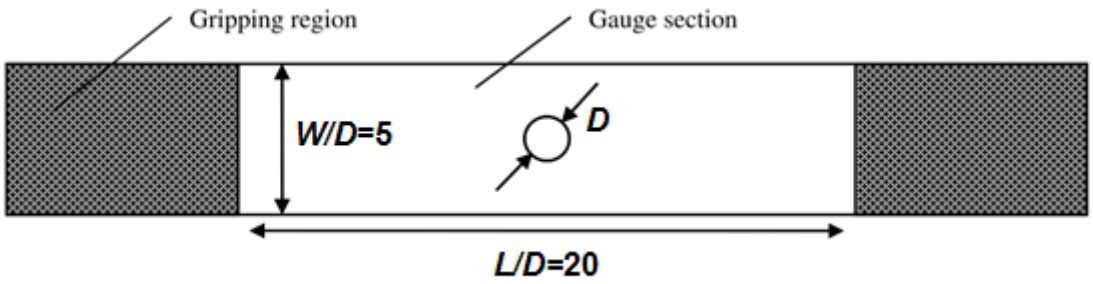

Figure 1. Schematic of the previous in-plane scaled open-hole specimens [11].

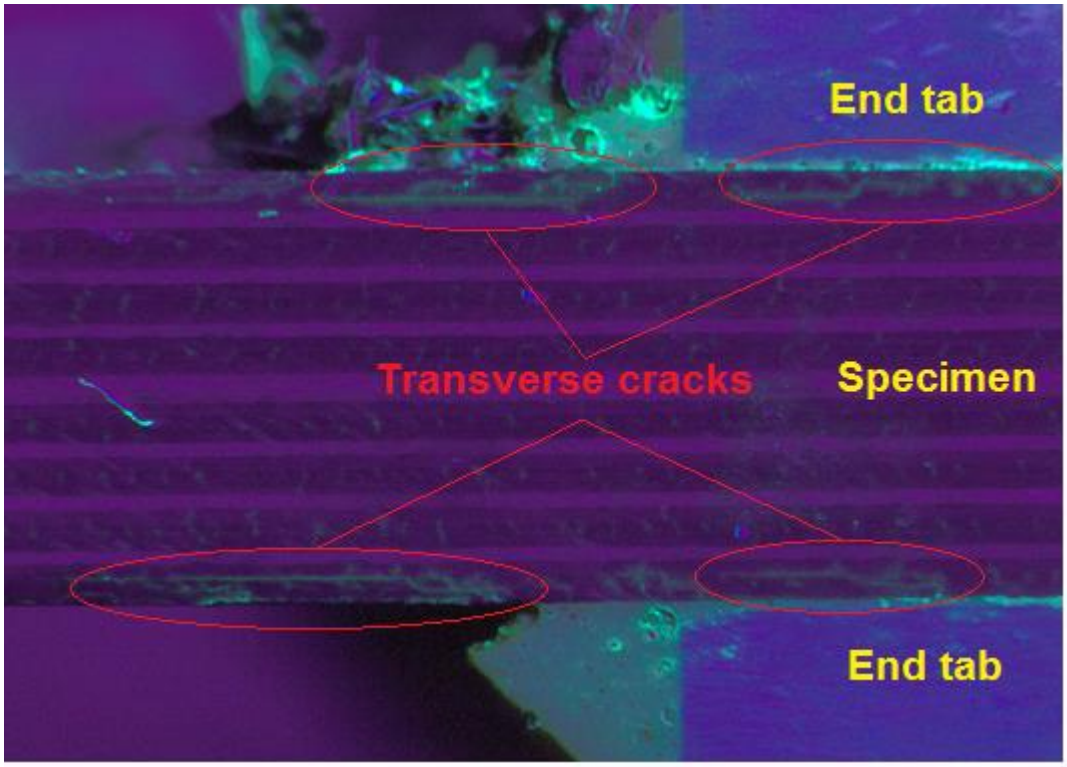

Figure 2. Transverse surface cracks starting at the end tabs at 95% of the average failure load.

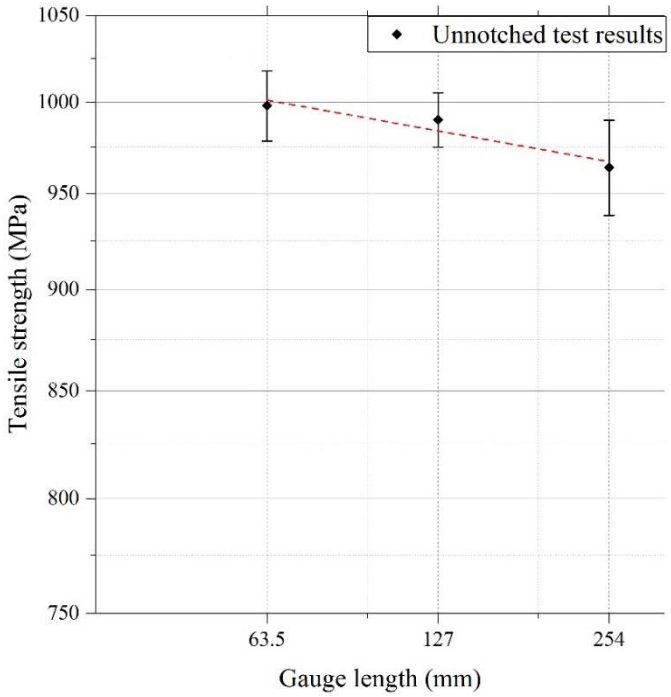

Figure 3. Size effects in length-scaled unnotched quasi-isotropic tests.

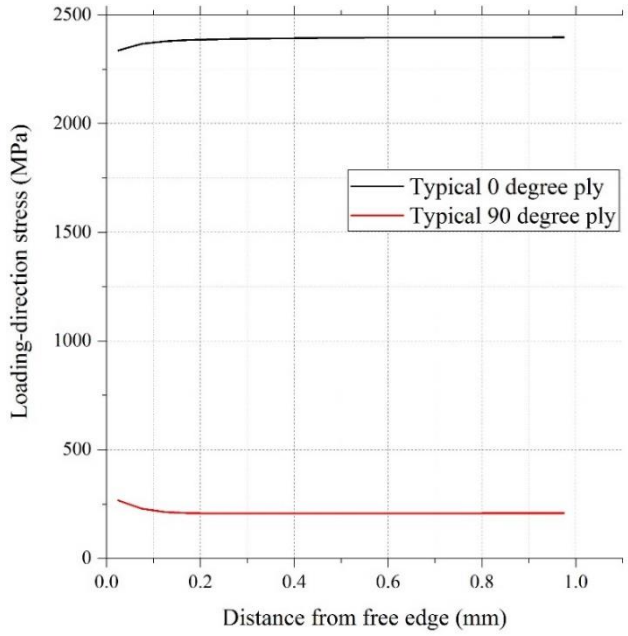

Figure 4. Free edge effects in the unnotched model with no damage.

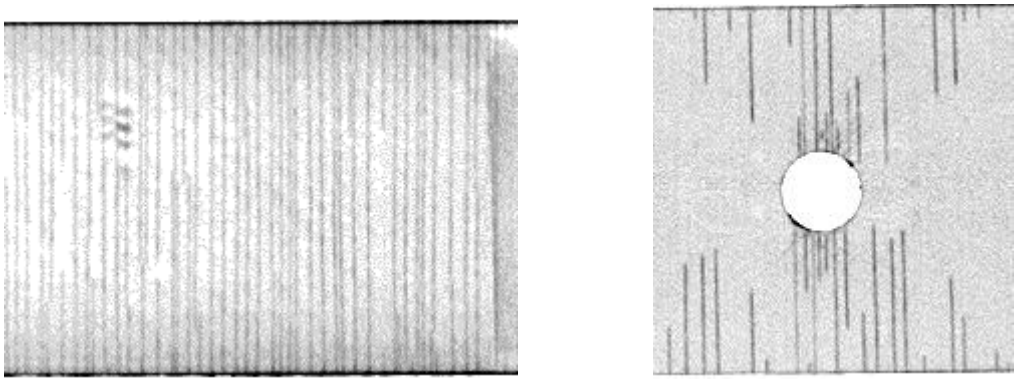

(a) Unnotched specimen (b) Open-hole specimen

Figure 5. Matrix cracks in 90° plies of quasi-isotropic laminates close to ultimate failure.

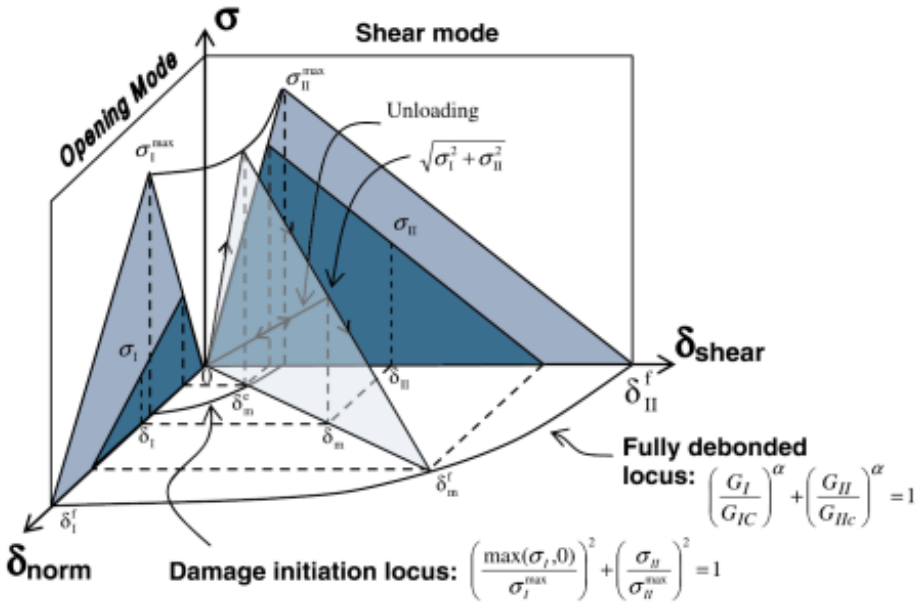

Figure 6. Mixed-mode traction displacement relationship for cohesive interface elements [23].

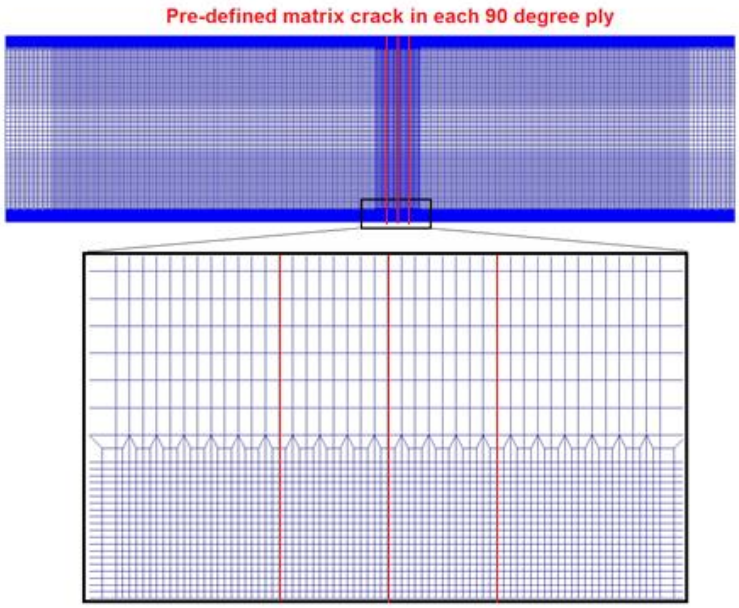

Figure 7. Unnotched FE model with three matrix cracks in each 90° ply (minimum mesh size of about 0.05 mm)

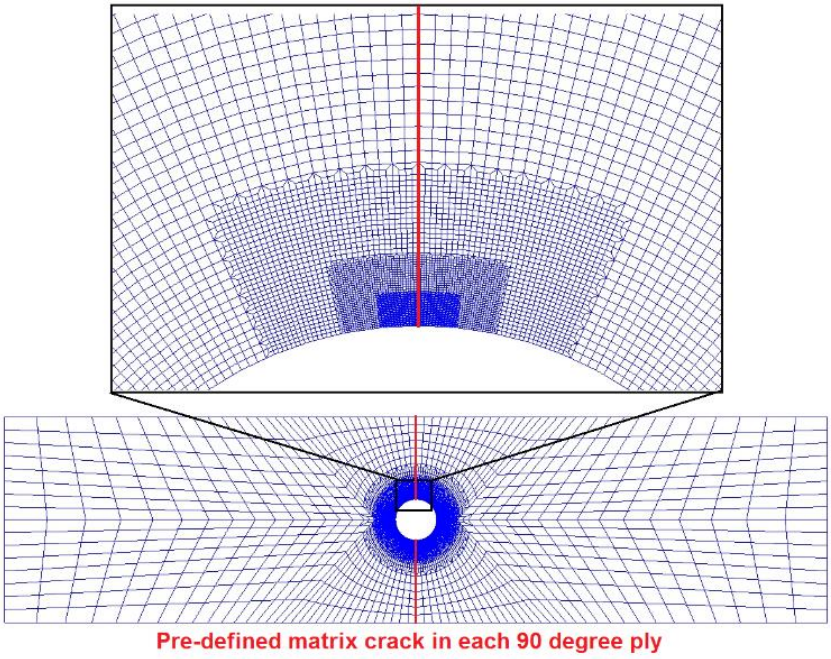

Figure 8. Scale 8 open-hole FE model with one matrix crack in each 90° ply (minimum mesh size of about 0.04 mm).

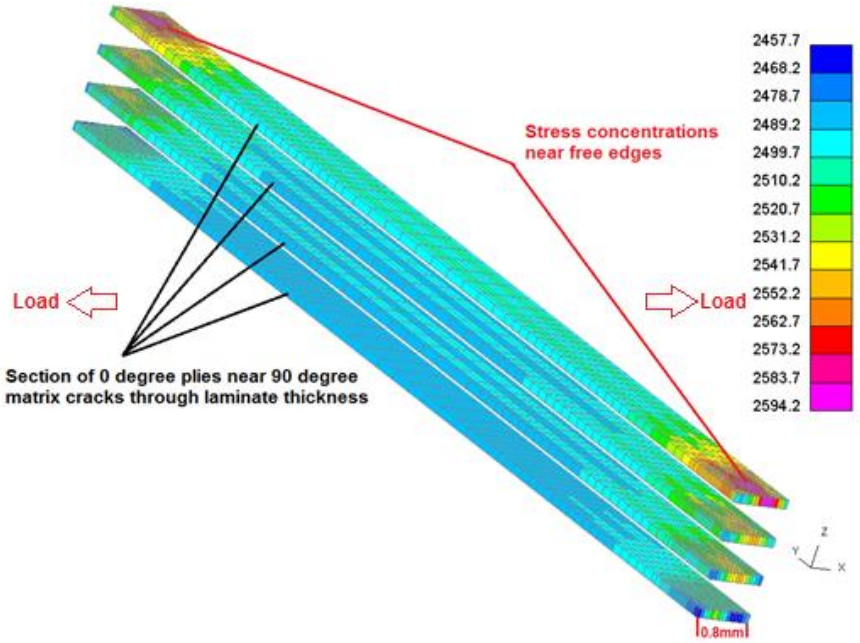

Figure 9. Loading-direction stress distribution in MPa in 0° plies close to ultimate failure with 90° matrix cracks across the full model width.

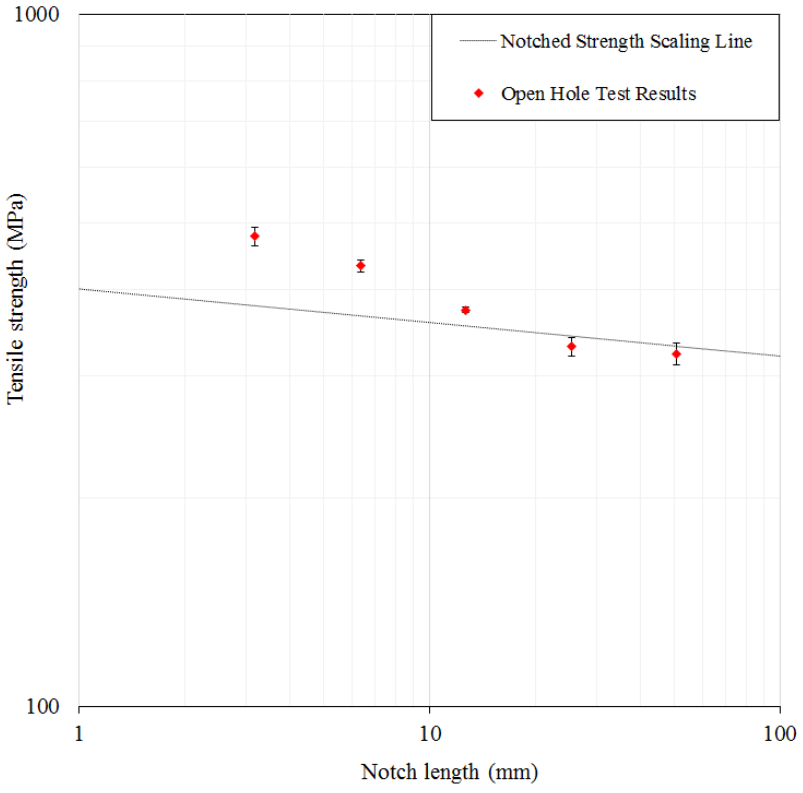

Figure 10. Notched strength scaling line for very large holes.

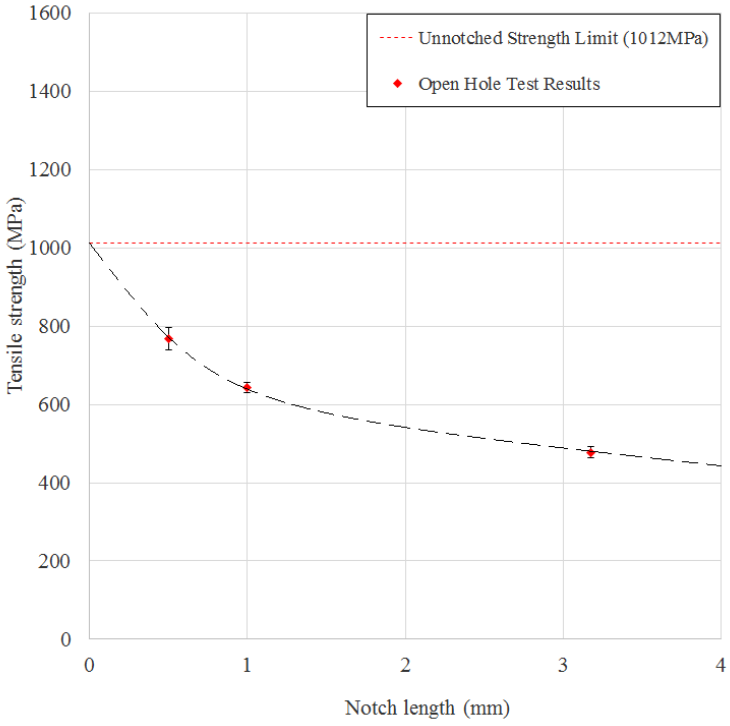

Figure 11. Notch sensitivity largely decreases for very small holes.

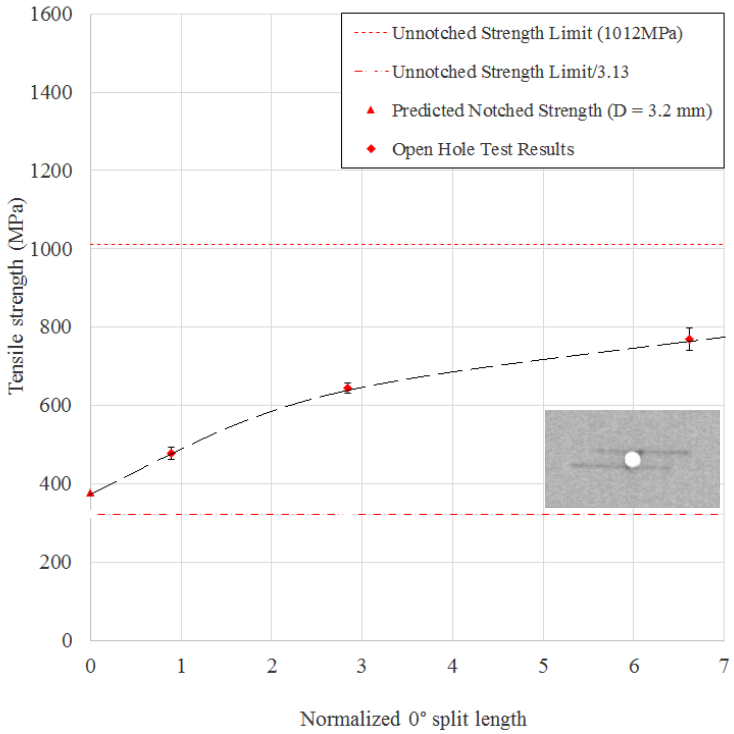

Figure 12. Notch sensitivity decreases with increasing normalized 0° split length, with a CT scanning image of the central 0° splitting for the 0.5 mm hole.

Table 1. Dimensions of the length-scaled unnotched quasi-isotropic specimens (mm).

Specimens	Gauge width	Gauge length
Short	16.2	63.5
Medium	16.2	127.0
Long	16.2	254.0

Table 2. Dimensions of the in-plane scaled open-hole quasi-isotropic specimens (mm).

Specimens	Hole diameter	Gauge width	Gauge length
Scale 0.5†	0.5	16.2	63.5
Scale 1.0†	1.0	16.2	63.5
Baseline	3.2	15.9	63.5
Scale 2	6.4	31.8	127.0
Scale 4	12.7	63.5	254.0
Scale 8	25.4	127.0	508.0
Scale 16‡	50.8	254.0	508.0

† Their in-plane dimensions were kept the same as the previous baseline specimen (D = 3.2 mm);

‡ Only their width and hole diameter of the specimen were scaled up, while the gauge length of the specimen being kept the same as the one-size-smaller Scale 8 specimen (D = 25.4 mm).

Table 3. Length-scaled unnotched quasi-isotropic tensile test results.

Gauge length (mm)	Unnotched test results (MPa) (C.V., %)	Predicted equivalent strength (MPa)	Difference %	Weibull modulus
63.5	998 (2.0)	1012	1.4	
127.0	990 (1.5)	995	0.5	40
254.0	964 (2.7)	979	1.5	

Table 4. Open-hole quasi-isotropic tensile test results.

Specimens	Hole diameter (mm)	Strength (MPa) (C.V., %)
Scale 0.5	0.5	769* (3.7)
Scale 1.0	1.0	644* (2.0)
Baseline [11]	3.2	478 (3.1)
Scale 2 [11]	6.4	433 (2.0)
Scale 4 [11]	12.7	374 (1.0)
Scale 8 [11]	25.4	331 (3.0)
Scale 16 [13]	50.8	323 (3.7)

*Open-hole strengths converted to the values under a notch-to-width ratio $\lambda = 0.2$, in order to be consistent with the previous specimens.

Table 5. Lamina properties of IM7/8552 [15].

ρ	E_{11}	$E_{22}=E_{33}$	$G_{12}=G_{13}$	G_{23}	$\upsilon_{12}=\upsilon_{13}$	υ_{23}	$\alpha_2=\alpha_3$	α_1
(ton/mm^3)	(GPa)	(GPa)	(GPa)	(GPa)			(℃$^{-1}$)	(℃$^{-1}$)
10^{-5}	161	11.4	5.17	3.98	0.320	0.436	3×10^{-5}	0.0

Table 6. Cohesive interface element properties of IM7/8552 [15].

G_{IC} (N/mm)	G_{IIC} (N/mm)	σ_I^{max} (MPa)	σ_{II}^{max} (MPa)	α
0.2	1.0	60	90	1.0